Journal of Cellular Biochemistry 96:1231–1243 (2005)

Differential Activation of Stress-Responsive Signalling Proteins Associated With Altered Loading in a Rat Skeletal Muscle

Inho Choi,[1]* Kisoo Lee,[1] Myungjoo Kim,[1] Moonyong Lee,[1] and Kyoungsook Park[2]**

[1]Department of Life Science, College of Liberal Arts and Science, Yonsei University, Wonju, Republic of Korea
[2]Molecular Therapy Research Center, Sungkyunkwan University, Seoul, Korea

Abstract Skeletal muscle undergoes a significant reduction in tension upon unloading. To explore intracellular signalling mechanisms underlying this phenomenon, we investigated twitch tension, the ratio of actin/myosin filaments, and activities of key signalling molecules in rat soleus muscle during a 3-week hindlimb suspension and 2-week reloading. Twitch tension and myofilament ratio (actin/myosin) gradually decreased during unloading but progressively recovered to initial levels during reloading. To study the involvement of stress-responsive signalling proteins during these changes, the activities of protein kinase C alpha (PKCα) and three mitogen-activated protein kinases (MAPKs)—c-Jun NH_2-terminal kinase (JNK), extracellular signal-regulated protein kinase (ERK), and p38 MAPK—were examined using immunoblotting and immune complex kinase assays. PKCα phosphorylation correlated positively with the tension (Pearson's $r = 0.97$, $P < 0.001$) and the myofilament ratio ($r = 0.83$, $P < 0.01$) over the entire unloading and reloading period. Treatment of the soleus muscle with a PKC activator resulted in a similar paralleled increment in both PKCα phosphorylation and the α-sarcomeric actin expression. The three MAPKs differed in the pattern of activation in that JNK activity peaked only for the first hours of reloading, whereas ERK and p38 MAPK activities remained elevated during reloading. These results suggest that PKCα may play a pivotal role in converting loading stress to intracellular changes in contractile proteins that determine muscle tension. Differential activation of MAPKs may also help alleviate muscle damage, modulate energy transport and/or regulate the expression of contractile proteins upon altered loading. J. Cell. Biochem. 96: 1231–1243, 2005.

Key words: alpha actin; MAPK; myofilament; PKC; reloading; twitch tension; unloading

A postural or antigravity muscle undergoes significant atrophy during spaceflight or hindlimb suspension. The atrophy is caused by considerable loss of cellular components (proteins and organelles) and extracellular fluid from the muscle [Fitts et al., 2001]. The most serious consequence of these changes is decreased muscle tension [Caiozzo et al., 1996]. This muscular problem has been a central issue in space biology because astronauts can face serious locomotor problems during an emergency in space or after return to Earth [Baldwin, 1996]. Various cellular and molecular factors are known to alter muscle contraction upon changes in loading [Vandenburgh et al., 1999; Baewer et al., 2004], yet the intracellular signalling mechanisms underlying this phenomenon remain unclear.

Weight loading imposes continuous contractile stress and physical stretch to postural muscles [Baewer et al., 2004]. This loading is crucial for maintaining muscle proteins and myofibrillar integrity, while its abnormal displacement causes various pathological problems including musculo-skeletal diseases

Grant sponsor: Basic Research Program of the Korea Science and Engineering Foundation (to IC); Grant number: R05-2003-000-10589-0.

*Correspondence to: Dr. Inho Choi, Department of Life Science, College of Liberal Arts and Science, Yonsei University, 234 Maeji-Ri, Heungup-Myon, Wonju, Gangwon-do 222-710, Republic of Korea.
E-mail: ichoi@dragon.yonsei.ac.kr

**Correspondence to: Kyoungsook Park, Molecular Therapy Research Center, Sungkyunkwan University, Samsung Medical Center Annex 8F, 50 Ilwon-Dong, Gangnam-Gu, Seoul 135-710, Republic of Korea.
E-mail: hannah05@dreamwiz.com

Received 19 July 2005; Accepted 25 July 2005
DOI 10.1002/jcb.20616

[Ingber, 2003; Hornberger and Esser, 2004]. If the muscle is unloaded, then it progressively loses myofibrillar proteins, with a concomitant decrease in protein synthesis and an increase in protein degradation [Vandenburgh et al., 1999; Isfort et al., 2002]. Consequently, the muscle wastes both actin and myosin, causing significant misalignment of myofilaments as well as a reduction in the number of cross-bridges [Riley et al., 2000; Adams et al., 2003]. If the muscle is reloaded, however, the tissue regains myofibrillar proteins and tension production, although it is uncertain whether the recovery mechanism is the reverse of the atrophic process. Thus, to better understand the muscle tension problem, we need to investigate how the expression of these proteins is regulated by intracellular mechanisms upon unloading and reloading (UR), which may virtually explain the extent of the alteration of myofibrillar integrity. A number of studies have investigated the signalling mechanisms in overloaded skeletal muscle (e.g., exercise) [Donsmark et al., 2003; Long et al., 2004]. However, few studies have addressed the signalling mechanisms in unloaded muscle.

According to previous reports, loading stress or stretch can be directly transduced into the cytoplasm through G protein-coupled receptors (GPCRs), Ca^{2+} channels and integrins in the cell membrane [Li and Xu, 2000; Ingber, 2003]. Once transduced, these stimuli selectively activate stress-activated signalling molecules and subsequent nuclear transcription of the relevant protein-coding genes. The primary candidate signalling pathways are those involving protein kinase C (PKC) and mitogen-activated protein kinases (MAPKs). PKCs are ubiquitous serine/threonine protein kinases that are involved in cell proliferation, regeneration and stress responses [Liu, 1996; Korzick et al., 2004]. To date, 12 PKC isoforms have been identified and classified into 3 subfamilies (conventional, novel and atypical), depending on their requirements for Ca^{2+} and diacylglycerol (DAG) derived from phosphatidylinositol-4,5-bisphosphate (PIP2) [Gutkind, 1998]. MAPKs are a family of serine/threonine kinases that include c-Jun NH_2-terminal kinase (JNK), p38 MAPK and extracellular signal-regulated protein kinase (ERK). As a part of downstream substrates of PKCs, MAPKs regulate muscle cell death, survival and regeneration, particularly in response to various stresses like oxidative stress, inflammation, stretch and exercise overloading [Boppart et al., 2000; Widegren et al., 2001; Donovan et al., 2002].

Previous studies demonstrate that the activation of PKC isoforms and MAPKs vary with the nature of the stress. For instance, denervation of skeletal muscle increases or decreases phosphorylation of a conventional PKCα or novel PKCθ, respectively [Sneddon et al., 2000], whereas exercise elevates the activation of atypical rather than conventional and novel PKCs [Rose et al., 2004]. Activation of the MAPKs appears to be more complicated because the levels of activation vary in a stimulus intensity- and duration-dependent manner [Long et al., 2004]. The JNK pathway is activated rather rapidly and transiently in injury-evoking exercise, whereas the activation of the ERK and p38 MAPK pathways may be associated with energy transport and/or cytoskeletal actin reorganisation during muscle contraction [Boppart et al., 2000; Donsmark et al., 2003]. The link between these kinases and PKCs has remained obscure, although some metabolism and myogenesis studies have demonstrated such a link [Long et al., 2004].

Based on the work described above, we explored the muscle tension problem by investigating the link between the external loading stress and signalling pathways that may regulate contractile protein expression. We attempted twitch tension measurements because this contraction occurs only within 1 s, hence allowing us to focus on the muscle contractile machinery and removing the potential effects of other factors (e.g., energy generation capacity) on muscle tension [Cain et al., 1962]. In addition, because muscle contraction increases the levels of both DAG and intracellular Ca^{2+}, and elevated DAG or treatment with phorbol ester enhances tension production [Ikebe and Brozovich, 1996; Donsmark et al., 2003], we considered that the phosphorylation of conventional PKC isoforms (cPKCs; α, β, γ) as a part of the key signalling processes underlying myofibrillar integrity.

On the basis of this rationale and the aforementioned studies, we hypothesised that phosphorylation levels of cPKCs positively correlate with twitch tension and myofibrillar integrity, with a decreasing and increasing trend during unloading and reloading, respectively. We also hypothesised that the activities of MAPKs decrease with unloading but rapidly increase

upon reloading (as in exercise), with the ERK and p38 MAPK pathways, rather than the JNK pathway, better linked to cPKC activation. We tested these hypotheses by examining changes in twitch tension, the ratio of actin/myosin filaments, and phosphorylation levels of cPKCs relative to expression of the α-sarcomeric actin level, and activities of MAPKs in the rat soleus muscle during 3 weeks of unloading and 2 weeks of reloading.

MATERIALS AND METHODS

Subjects

All studies involving animals were approved by the Yonsei University Animal Care and Use Committee. Sprague-Dawley rats (5 weeks old, 100–120 g) were maintained at 22–24°C in a 14:10 h light:dark cycle. Standard Purina rat chow and water were provided ad libitum. On the last day of week 5, the rats were randomly divided into seven groups: two unloading groups of 1 week (U1w) and 3 week (U3w); four reloading groups, which experienced the 3 week unloading followed by 1 h, 5 h, 1 day or 2 week reloading (R1h, R5h, R1d and R2w, respectively); and one representative age-matched control group kept for 3 weeks under standard conditions (C3w). We did not include C5w (an age-matched control for R2w) because muscle contractile properties and myofilament structure do not differ between C3w and C5w [Lee et al., 2004]. We used a modified model of hindlimb suspension adopted from Nyhan et al. [2002]. Each animal was caged separately and anaesthetised intraperitoneally with pentobarbital sodium (30 mg/kg). Two pieces of flexible Tygon tubing (5.6 mm OD) were placed along the dorsum of the animal and were sutured with silk threads to provide a firm support. On the following day (the first day of week 6), after the animal recovered completely from the anaesthetics, the tubing at the tip of the tail was connected to a tether so that the animal was suspended at an incline of 35° in a head-down orientation. The animal was free to move around the cage on its front feet. The mesh jacket was replaced in 7–10 days as the animal grew. Similar tubing and jackets were applied to the control groups with the exception that the tail was not taped to the tubing. At the time of reloading, the animals were freed from all tubing and jackets and were housed in individual cages.

Twitch Contraction

On the day of experiment, each subject was anaesthetised with pentobarbital sodium (i.p., 50 mg/kg), and the soleus muscles of both hindlimbs were quickly removed. The left limb muscle was frozen immediately in liquid nitrogen for immunoblotting and immune complex kinase assays or in 2.5% glutaraldehyde for electron microscopy (EM). The right limb muscle was soaked in 70 ml of oxygenated Ringer's solution (115 mM NaCl, 5 mM KCl, 4 mM $CaCl_2$, 1 mM $MgCl_2$, 1 mM NaH_2PO_4, 24 mM $NaHCO_3$, 11 mM glucose, 0.02 g/L tubocurarine chloride, pH 7.39) at 25°C. One tendon was tied to a lever arm of a 300B-LR servomotor system (Aurora Scientific, Aurora, Canada), and the other tendon was tied to a micrometer to adjust to the optimal muscle length (L_o). A custom DMC program (Aurora Scientific) was used to control both the servo system and a Grass S48 stimulator. The stimulator was connected to a pair of bright platinum electrodes and supplied a 1.0-ms square wave pulse that generated maximum twitch force. At the completion of the twitch experiment, the tissue was frozen in place at L_o with liquid nitrogen, sectioned (8 μm) in a Microm HM505E cryostat, and stained by a routine haematoxylin and eosin procedure. The cross-sectional area (CSA) of each muscle was determined as described previously [Lee et al., 2004]. The force data were analysed by custom software (DMA, Aurora Scientific) and normalised to the CSA.

Electron Microscopy

The soleus muscles used in the EM study were obtained from three rats per group. Each tissue was pre-fixed for 4 h in 2.5% glutaraldehyde, cut into $1 \times 1 \times 2$ mm blocks, rinsed for 15 min in 0.1 M phosphate buffer (pH 7.2) and post-fixed for 2 h in 1% OsO_4. The fixation and rinsing processes were conducted at 4°C to minimise autolysis and extraction. The fixed samples were dehydrated two times in a series of ethanol solutions (50%, 60%, 70%, 90% and 100%). The samples then were infiltrated with propylene oxide, affixed sequentially on dodecenyl succinic anhydride, epon 812, nadic methyl anhydride and tri(dimethylaminomethyl) phenol (DMP-30) for 1 h each at room temperature and then polymerised at 60°C overnight. After trimming and semi-thin sectioning, muscle samples were dried on a hot plate (80°C) and

were prestained with 0.5% toluidine blue. The semi-thin sections were trimmed, ultra-thin sectioned with an ultramicrotome and double-poststained with 1% uranyl acetate for 15 min and lead citrate for 5 min. Ultra-thin sections (0.05 μm) were supported on a grid. Cross-sections were adjusted to 120,000× magnification under an electron microscope (TEM, JEM-1200EX, Jeol, Tokyo, Japan), photographed by a digital TEM camera (Megaview III), and analysed using an Image Analysis System (SIS, Munster, Germany).

We chose three photographed images out of 12 images per tissue, in which both actin and myosin filaments were clearly evident. We divided each image into ~10 quadrates (63 nm × 63 nm each) using Adobe Photoshop 5.0 software (Adobe Systems, Inc., San Jose, CA), and randomly selected four quadrates. Actin and myosin filaments were then counted within each quadrate. Any actin or myosin filament appearing on the edge of the quadrate was not counted.

Immunoblotting and Immune Complex In Vitro Protein Kinase Assays

The frozen muscle tissues were homogenised in five volumes of tissue lysis buffer (25 mM HEPES, pH 7.5, 0.3 M NaCl, 1.5 mM $MgCl_2$, 0.2 mM EDTA, 0.05% (w/v) Triton X-100, 20 mM β-glycerophosphate, 0.1 mM orthovanadate, 0.5 mM DTT, 0.4 mM phenylmethylsulfonyl fluoride (PMSF), 1 g/ml leupeptin, 1 g/ml pepstatin), as described previously [Lee et al., 2002]. After a 15-min incubation on ice, tissue lysates were centrifuged at 12,000 rpm using a microcentrifuge for 15 min at 4°C. The supernatant was saved as the whole-tissue soluble lysate. The Bradford assay was used to determine the protein concentration in lysates according to the manufacturer's protocol (Bio-Rad, Hercules, CA). Whole-tissue lysates (50 μg) were subjected to SDS–PAGE on 10% gels followed by electrophoretic transfer of protein bands to a nitrocellulose membrane and subsequent incubation with three antibodies against cPKCs (PKCα, PKCβ, PKCγ). Immune complexes were detected with the ECL system (Amersham Pharmacia Biotech, Uppsala, Sweden) and quantitated using a densitometer (Gel document, Bio-Rad). The loading and transfer of protein was normalised to β-tubulin. The activities of MAPKs (JNK, ERK, p38) were determined by immune complex kinase assays, as described previously [Lee et al., 2002]. Protein from soluble lysates (500 μg) was incubated with specific antibodies against JNK, ERK or p38 MAPK for 2 h at 4°C. Immunoprecipitation was achieved using a 1-h incubation with protein G-Sepharose. Immune complexes were washed twice with Triton X-100 lysis buffer and three times with 20 mM HEPES (pH 7.4), and resuspended in 20 μl of kinase assay buffer containing 10 mM $MgCl_2$, 2 mM DTT, 0.2 mM sodium orthovanadate and 2 μg of substrate. GST-c-Jun, GST-ATF2 or MBP was used as a substrate for JNK, p38 or ERK, respectively. The MAPK activity assays were carried out in the presence of 20 μM unlabeled ATP and 2 μCi of [γ-^{32}P]ATP for 30 min at 30°C and terminated by the addition of 5 μl of 5 ml SDS sample buffer and boiling for 5 min. The reactions were separated by SDS–PAGE on a 15% gel. The phosphorylation of the substrate proteins was examined by autoradiography and quantitated using a densitometer (Gel document, Bio-Rad). The same blot was used to examine an equal load of immunoprecipitated JNK, ERK and p38 MAPK by incubation with the corresponding antibody. Antisera and substrates used for immune complex assays were: PKC antibody sampler kit (anti-PKCα, anti-PKCβ and anti-PKCγ) from Transduction Labs (Lexington, KY); anti-JNK, anti-ERK (1/2), and anti-p38 from Santa Cruz Biotechnology (Santa Cruz, CA); GST-c-Jun, GST-ATF2, from New England Biolabs (Beverly, MA); myelin basic protein (MBP) from Sigma (St. Louis, MO); anti-phosphorylated PKCα at Ser^{657} from Upstate Biotechnology (Charlottesville, VA); and protein G-Sepharose and [γ-^{32}P]ATP (specific activity, 5,000 Ci/mmol) from Amersham Pharmacia. The secondary antibodies were horseradish peroxidase-conjugated anti-rabbit IgG or anti-mouse IgG from Zymed (San Francisco, CA).

Activation of PKCα Ex Vivo and Expression of α-Actin

To explore correlation between PKCα activation and expression of α-sarcomeric actin, soleus muscles were dissected from 6-week-old rats and then incubated ex vivo with the PKC activator, phorbol 12-myristate 13-acetate (PMA, 100 nM, Sigma), dissolved in 100% dimethyl sulfoxide (DMSO) for various periods (0, 0.5, 1, 2, 5 h) at pH 7.39, 25°C. The muscle tissues were then homogenised in five volumes of tissue lysis buffer (described above) to

prepare whole-tissue lysates. Phosphorylation of PKCα and expression of α-actin were determined by immunoblotting with anti-phosphorylated PKCα antibody (Ser^{657}) and anti-α-actin antibody (Sigma), respectively.

Data Presentation

All data are presented as the mean ± 1SEM, or as otherwise noted. Significance of intergroup differences was examined by one-way analysis of variance (ANOVA) and Bonferroni's post hoc test. Correlations among twitch tension, actin/myosin ratio, and activities of signalling proteins, and also between PKCα phosphorylation and α-actin levels were determined by Pearson's coefficients (r), and the significance was examined by the two-tailed *t*-test on r. The statistics were performed with SPSS/PC+ at the significance level $P = 0.05$.

RESULTS

Body Mass and Muscle Mass

Body mass and muscle properties for the control and the UR groups are summarised in Table I. As expected, muscle mass relative to body mass decreased by 39.8% in U3w but recovered to the control level in R2w ($P < 0.001$; Fig. 1A). Muscle CSA also decreased by 43.9% in U3w but increased to 122.1% of the control in R2w ($P < 0.001$; Table I).

Twitch Tension

Figure 1B and C presents the maximum twitch force and twitch tension, respectively, of the soleus muscle for each loading condition. Twitch force of C3w was 10.2 ± 0.8 g; this force decreased by 61.5% in U3w and 62.4% in R5h, and returned to 128% of the control in R2w ($P < 0.001$). Twitch tension of C3w was 39.2 ± 2.8 mN/mm^2; this tension decreased significantly by 34.1% in U3w and 37.3% in R1h, and returned to 96.4% of the control in R2w ($P < 0.001$). Twitch rise time between onset and the point of peak force ranged from 23 to 46 ms for all controls and UR groups examined.

Electron Microscopic Analysis

Figure 2A–D illustrates representative electron micrographs of cells in cross-sectioned soleus muscles for groups C3w, U3w, R1h and R2w. In C3w, actin filaments were fairly well organised in a hexagonal array around each myosin filament, whereas in U3w and R1h the actin arrangement was somewhat irregular. In R2w, the number of actin filaments around each myosin filament was greater than that in C3w.

Since the magnification of the micrographs was the same, the numbers of actin and myosin filaments in each quadrate were counted. Figure 3A and B presents the average number of actin filaments per quadrate and the ratio of actin/myosin filaments for each loading condition. Each quadrate contained 24–33 myosin filaments, depending on the loading status of the muscle. Actin and myosin filaments were differentially affected by the loading conditions in that the decrease in the number of actin filaments was greater than that of myosin filaments, with the lowest value at R1h. As a result, the actin/myosin filament ratio reduced significantly upon the loading status from 3.65 in C3w, 2.00 in R1h and 4.01 in R2w ($F_{6,143} = 84.08$, $P < 0.001$).

Phosphorylation of cPKC Isoforms

Since muscle contractility depends on Ca^{2+} concentration, we examined the phosphorylation status of three conventional PKC isoforms (α, β, γ) in soleus whole-tissue lysates using

TABLE I. Summary of Morphological Analysis of the Rat Soleus Muscle During Unloading and Reloading Conditions

Groups	C3w	U1w	U3w	R1h	R5h	R1d	R2w
Variables							
Body mass (g)[a]	269.88 ± 3.12	202.57 ± 6.89	230.20 ± 7.06	227.84 ± 6.31	223.72 ± 10.91	230.49 ± 11.92	358.91 ± 23.54
Muscle mass (g)[b]	0.107 ± 0.009	0.076 ± 0.004	0.054 ± 0.005	0.057 ± 0.004	0.058 ± 0.005	0.061 ± 0.002	0.141 ± 0.008
Cross-sectional area (CSA) (mm^2)[c]	4.142 ± 0.281	3.249 ± 0.220	2.355 ± 0.189	2.340 ± 0.149	2.318 ± 0.228	2.621 ± 0.096	5.102 ± 0.262

Values are mean ± 1SEM.
[a]The value of C3w differed significantly from those of U1w and R2w; the value of R2w differed significantly from all others (one-way analysis of variance (ANOVA) and Bonferroni's post hoc test; $F_{6,53} = 19.8$, $P < 0.001$).
[b]Values differed significantly between all pairs of groups ($F_{6,53} = 38.1$, $P < 0.001$).
[c]The value of C3w differed significantly from those of U3w, R1h, R5h, R1d and R2w; the value of R2w differed significantly from all others ($F_{6,53} = 23.3$, $P < 0.001$).

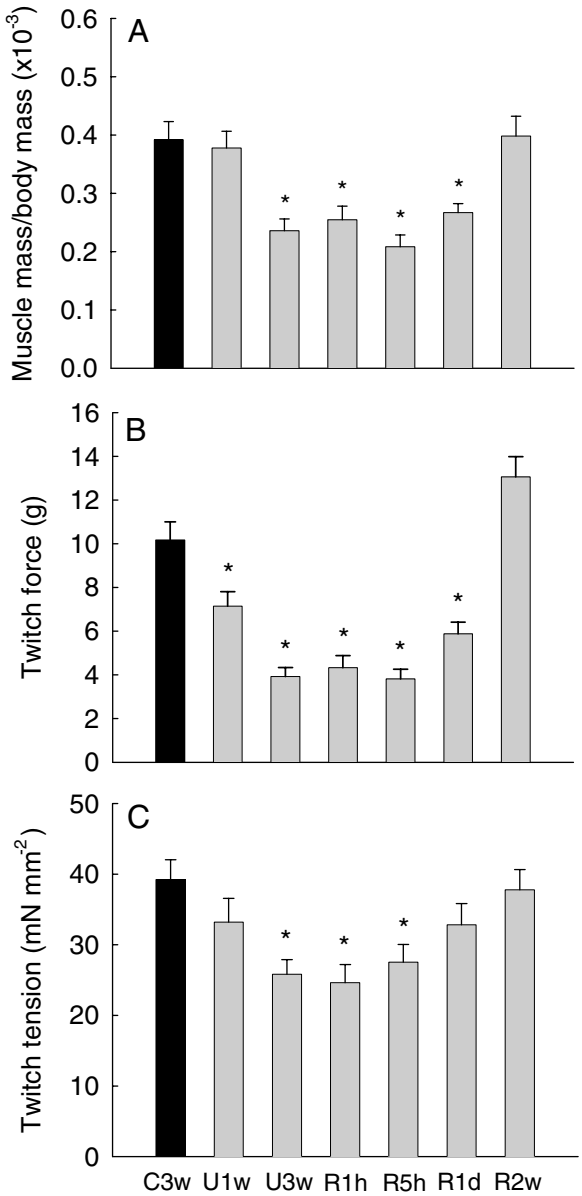

Fig. 1. The soleus muscle undergoes significant atrophy and a reduction in tension during unloading, but recovers to the initial levels as reloading proceeds. **A**: Soleus muscle mass relative to body mass, (**B**) maximum twitch force and (**C**) normalised tension are illustrated for each loading condition. Twitch force was generated at 25°C by a 1.0-ms pulse at supramaximal voltage and was normalised by the cross-sectional area (CSA) of the tissue. Each data point represents the mean ± 1SEM; n = 15 for C3w, and n = 9 for unloading or reloading groups. *Significantly different from both C3w and R2w (one-way analysis of variance (ANOVA) and Bonferroni's post hoc test, $P < 0.05$).

corresponding phospho-PKC-specific antibodies. Compared with the control, PKCα phosphorylation levels decreased steadily to 67.3% at U3w, 62.4% at R1h and then returned to 89.4% at R2w (n = 6, $P < 0.01$) (Fig. 4A and B). In contrast, our preliminary results had revealed that expression of both PKCβ and PKCγ as well as phosphorylation levels of PKCβ and PKCγ were at the limit of detection in our rat muscle tissues, making it difficult to accurately calculate any variation among the groups (data not shown). Since PKCα was the prominent isoform detected in our study, we next examined the correlation between PKCα and α-actin expression in soleus strips after treatment with 100 nM PMA, a PKC activator, over four different time periods (n = 6 for each). PMA treatment induced significant PKC phosphorylation at 30 min post-treatment, which then decreased gradually over the next 4.5 h ($P < 0.05$). A similar pattern of induction was observed for α-actin expression, with peak induction occurring at 1 h post-treatment ($P < 0.05$) (Fig. 4C and D). Taken together, the data indicate a significant correlation between PKCα phosphorylation and α-actin expression (Pearson's r = 0.51; $P < 0.05$) (Fig. 4E).

Changes in MAPK Activities

MAPKs are important for mediating intracellular signalling brought on by many types of stress. To explore the involvement of MAPKs in transmitting external loading signals in the soleus muscle, we used immune complex kinase assays (two samples per group) to examine changes in the temporal profiles of MAPK signalling activities in response to loading changes (Fig. 5A, C and E). The U1w samples were not included because preliminary studies showed that the activity of each MAPK in U1w was similar to that in C3w or U3w. Relative to the level of C3w, JNK activity increased dramatically 11.3 ± 4.9 fold in R1h and rapidly returned to the control level after R5h (Fig. 5B). ERK activity, however, remained similar to the control level until R1h and then increased after R5h, reaching a level 7.4 ± 2.7 fold that of the control in R2w (Fig. 5D). The activity of p38 MAPK, on the other hand, increased ~2.0 fold between R1h and R1d, and then decreased to 1.5 fold of the basal level in R2w (Fig. 5F).

Relationships Among Twitch Tension, Ratio of Actin/Myosin Filaments and PKCα Phosphorylation

Twitch tension, myofilament ratio and PKCα responses showed similar U-shaped trends across the UR period, and thus we conducted regression and correlation analyses between pairs of datasets (Table II). The regression slope

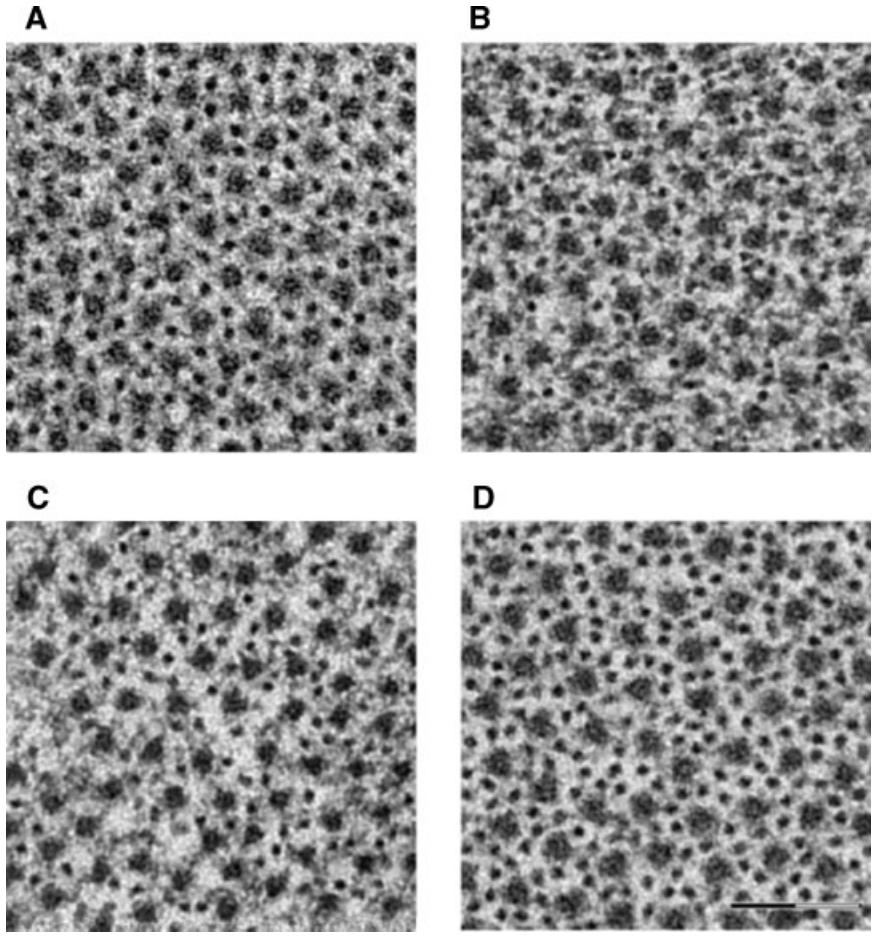

Fig. 2. The number of actin and myosin filaments in cross-sectioned soleus muscle cells changes markedly with the loading status, as shown in the representative electron micrographs for C3w (**A**), U3w (**B**), R1h (**C**) and R2w (**D**). Three soleus tissues from three subjects were used in each group, with four quadrates selected per section (totalling 24–36 quadrates per group). Each micrograph shown here is a single quadrate (63 nm × 63 nm), as used for quantitation in Figure 3.

between twitch tension with actin/myosin ratio was 0.97, and the correlation coefficient (Pearson's r) between these two variables was 0.88 ($P < 0.01$). The correlation coefficients between twitch tension and the PKCα phosphorylation and between the actin/myosin ratio and PKCα phosphorylation were 0.97 ($P < 0.001$) and 0.81 ($P = 0.028$), respectively.

DISCUSSION

In our experimental system, the twitch tension of the soleus muscle peaked in less than 0.1 s, under both normal and unloaded conditions. During this brief time, the muscle would utilise already-available phosphagens (ATP, creatine phosphate), which may be present in sufficient quantities in the sarcoplasm for simple cross-bridge turnover [Cain et al., 1962]. Therefore, the key factor directly limiting muscle tension must be the contractile machinery (e.g., myofibrillar components). From this baseline, the current study aimed to elucidate the stress-mediated signalling mechanisms that link external stimuli to tension capacity via myofibrillar alterations.

Our results show that there is a good correlation between twitch tension, the ratio of actin/myosin filaments and PKCα phosphorylation over the entire UR period. We also observed that three kinds of MAPKs (JNK, p38, ERK) are differentially regulated after reloading: Activation of JNK was rapid but transient only during early reloading; activation of ERK remained at the basal level for the first several hours of reloading and rapidly increased thereafter; and p38 MAPK was activated for at least 1 day after reloading. Thus, in general our results re-

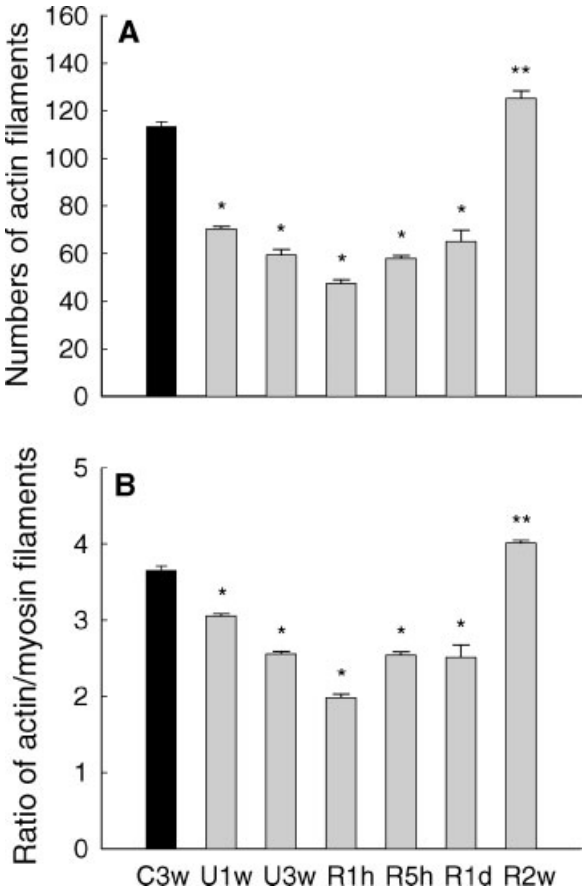

Fig. 3. Actin and myosin filaments are differentially affected by the loading stress. The number of actin filaments decreased more substantially than that of myosin filaments during unloading. **A**: The number of actin filaments per quadrate, and (**B**) the ratio of actin/myosin filaments are shown for each loading level. *Significantly different from both C3w and R2w; **significantly different from C3w (one-way ANOVA and Bonferroni's post hoc test, $P < 0.05$).

garding the relationships between PKC and myofibrillar integrity and muscle tension support our first hypothesis. The hypothesis regarding the temporal trends of MAPKs over the loading conditions as well as their molecular links with PKCα needs further investigation.

The soleus muscle lost a higher percentage of mass than did the whole body during the 3-week unloading period, indicating greater atrophy of the tissue compared with the rest of the body. The serious consequences of this atrophy were alterations in muscle tension and myofibrillar integrity (indicated by the ratio of actin/myosin filaments). The 34% decrease in the tension production capacity in our study is essentially the same as that (33%) reported previously [Caiozzo et al., 1996]. This tension reduction could be explained in part by a disproportional loss of actin filaments relative to myosin, such that the actin/myosin ratio decreased by 31% during the 3-week period (Fig. 3; also see Riley et al. [2000]). Importantly, the overall temporal trend of the myofilament ratio closely paralleled that of twitch tension during the UR period, with the regression slope near unity and a correlation coefficient of 0.88 (Table II). Because both the tension and actin/myosin ratio were measured on the basis of the muscle cross-section, the reduced tension must be the result of decreased numbers of cross-bridges per CSA, which must be directly affected by the loading status. The unexplained variation in the correlation (ca. 23%) might arise from several factors, such as misalignments between actin and myosin filaments or sarcomere lesions in the myofibres experiencing altered loading [Fitts et al., 2001].

Our next approach to the issue of muscle tension reduction was to understand how this myofibrillar alteration might be regulated by intracellular mechanisms that are linked to mechanical stimuli. As shown in Figure 4A and B, PKCα phosphorylation was significantly altered by the loading status. The levels of the other two cPKCs (β and γ) were too low to assess the loading effect. Low levels of these isoforms also have been reported in other studies on rodent skeletal muscle [Hilgenberg et al., 1996; Boczan et al., 2000; Goel and Dey, 2002]. Such responsiveness of PKCα to variable loading conditions could be anticipated considering the role of the soleus muscle on antigravity balance. Thus, under the normal loading, the PKCα is continually translocated from the sarcoplasm to the cell membrane and activated through binding with DAG and calcium (released from the sarcoplasmic reticulum) [Liu, 1996; Gutkind, 1998]. However, the signalling pathway could be down regulated during unloading and reactivated upon reloading.

This pattern of PKCα phosphorylation under different loading conditions may affect tension production in two ways: first, by regulating the expression of contractile proteins (the focus of our study), and second, by changing the biochemical properties of existing myofibrillar components (e.g., affecting Ca^{2+} sensitivity of myofilaments and myosin light chain phosphatase activity in smooth muscle) [Ikebe and Brozovich, 1996; Tanaka et al., 2002]. Regarding the first proposition, our data show that PKCα phosphorylation correlates well with both

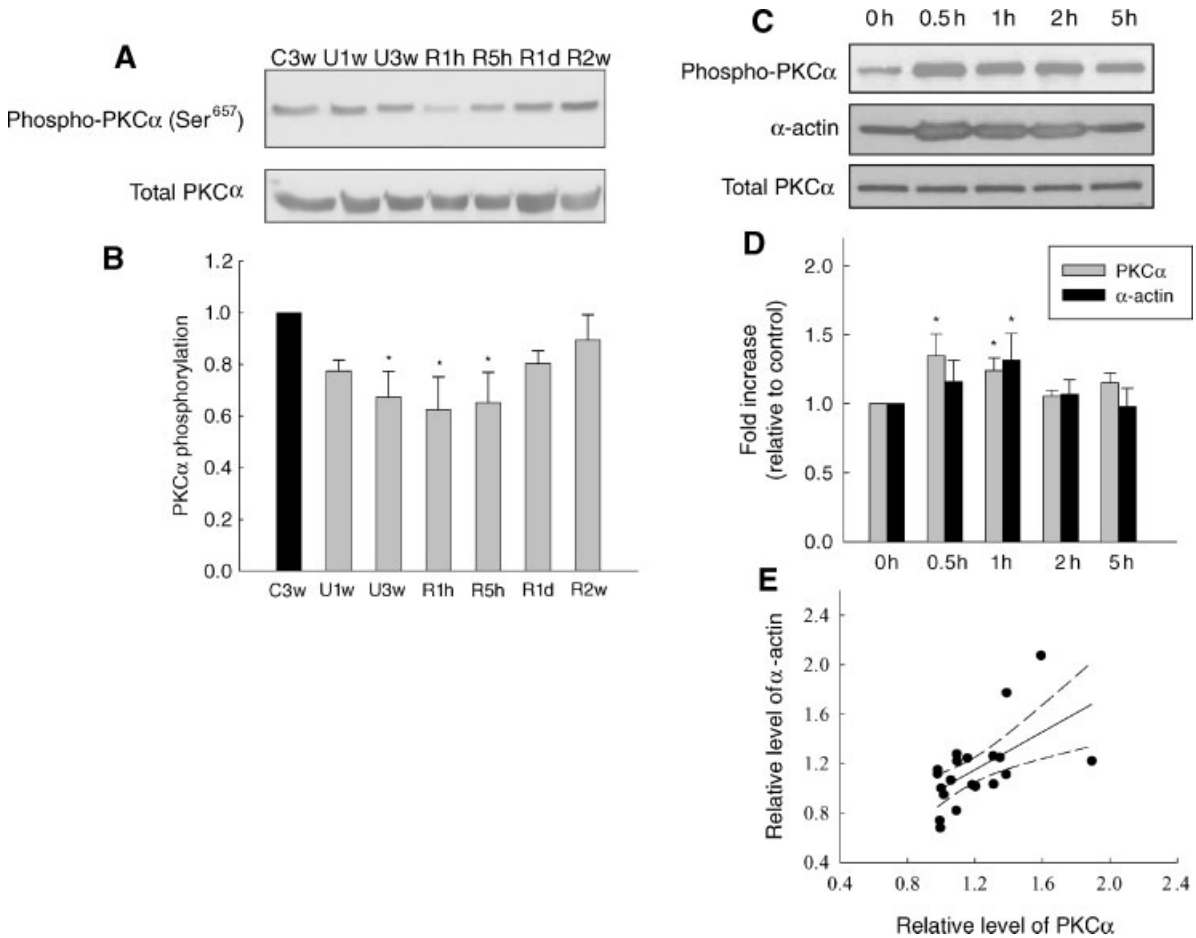

Fig. 4. The phosphorylation level of protein kinase C alpha (PKCα) decreases significantly during unloading and early reloading, but gradually recovers to the basal level as reloading proceeds. **A**: Immunoblot analysis of PKCα phosphorylation at Ser^{657}. Whole-tissue lysates were subjected to SDS–PAGE followed by incubation with a phospho-PKC(Ser^{657})-specific antibody. Total PKCα level was also measured by immunoblotting with an antibody against PKCα. **B**: Quantitation of PKCα phosphorylation. Phosphorylation levels are relative to that measured for C3w. Each data point represents the mean ± 1SEM (n = 6). *Significantly different from C3w (one-way ANOVA and Bonferroni post hoc test, $P < 0.01$). **C–D**: Association of PKCα phosphorylation with α-actin expression. Soleus muscles were treated with 100 nM phorbol 12-myristate 13-acetate (PMA) for the indicated period, and then the phosphorylation of PKCα and expression of α-sarcomeric actin were determined by immunoblotting with the indicated antibody. The same immunoblot was probed with a PKCα antibody to show equal loading. Each data point represents the mean ± 1SEM (n = 6). *Significantly different from 0 h (control) ($P < 0.05$). **E**: Regression and correlation analyses between PKCα phosphorylation and α-actin level obtained from the 100-nM PMA treatment experiment ($Y = 0.77X + 0.23$; Pearson's $r = 0.51$, $P < 0.05$).

the actin/myosin filament ratio (Table II) and α-actin levels (Fig. 4D and E). Upon treatment with the PKC activator, PMA, a 1.4 fold elevation of PKC phosphorylation was followed by a similar increase in α-actin expression. About a 30-min delay between peaks of two variables would be the time lag from the post-transmembrane to post-translational processes.

A cellular mechanism underlying functional association of PKCα and α-actin has yet to be clarified. Emerging evidence suggest that actin expression would depend on the cytoplasmic level of monomeric actins (G-actin) and behavior of PIP2 (the sarcolemmal secondary messenger) that responds to external stimulus [Lyubimova et al., 1997; Laux et al., 2000]. Synthesis of actin molecules was increased when the G-actin level was decreased during polymerisation of actin in various cells [Lyubimova et al., 1997; Laux et al., 2000]. Furthermore, PKC substrates like myristoylated alanine-rich C kinase substrate (MARCKS) were found to stimulate actin assembly by promoting clustering of PIP2 in the sarcolemma [Laux et al., 2000; Bittner and Holz, 2005]. It may thus be speculated that the external stress

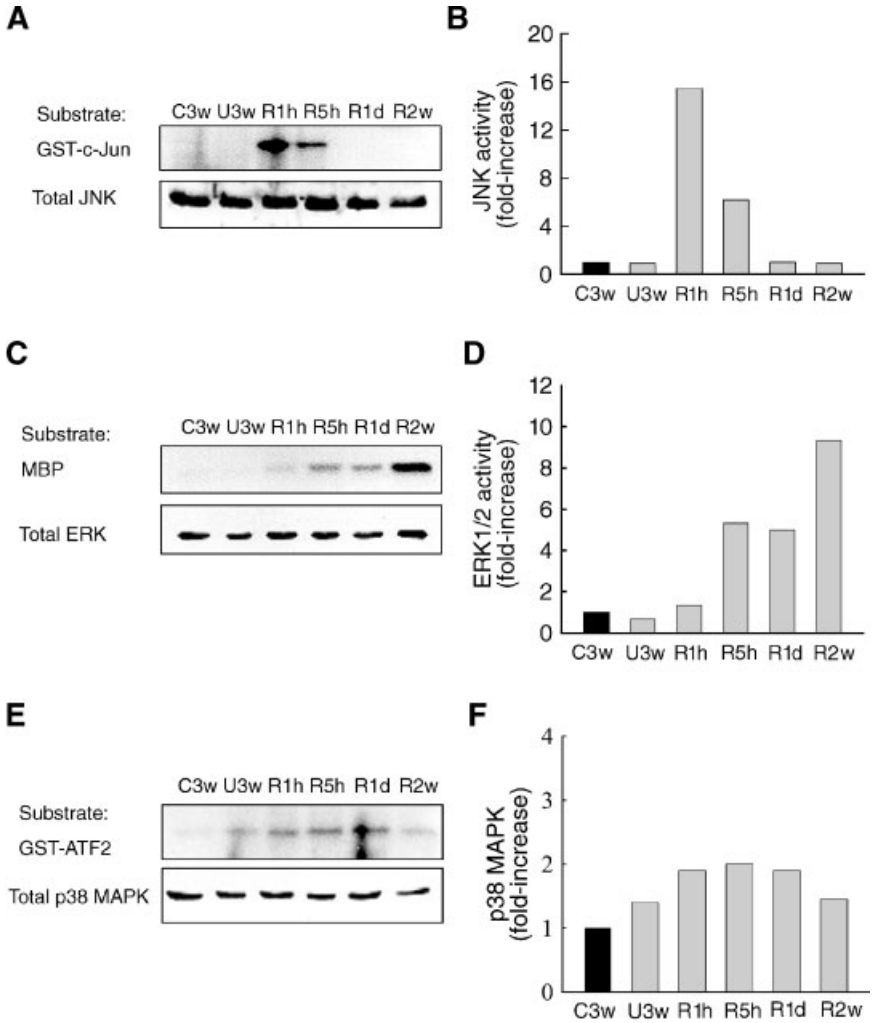

Fig. 5. The three mitogen-activated protein kinases (MAPKs) show differential activation upon altered loading stress. Whole-tissue soluble lysates were used to determine the activities of c-Jun NH_2-terminal kinase (JNK) (**A**, **B**), extracellular signal-regulated protein kinase (ERK) (**C**, **D**) and p38 MAPK (**E**, **F**) using immune complex kinase assays. Purified recombinant GST-c-Jun, MBP or GST-ATF-2 were used as substrates for JNK, ERK and p38 MAPK respectively. The levels of total JNK, ERK, p38 MAPK were measured by immunoblotting with respective antibodies. The levels changed little during the experiment. Two animals were used per group, and the data are representative of the two sample sets tested.

TABLE II. Regression and Correlation Analyses Among Twitch Tension, Myofilament Ratio and PKCα Phosphorylation

	X variables	
Y variables	Actin/myosin ratio	PKCα phosphorylation
Twitch tension		
Regression equation	$Y = 0.97\ X + 0.053$	$Y = 0.79\ X + 0.267$
Correlation coefficient[a]	$r = 0.877$	$r = 0.966$
Significance for r[a]	$P < 0.01$	$P < 0.001$
Actin/myosin ratio		
Regression equation	—	$Y = 0.85\ X - 0.024$
Correlation coefficient[a]		$r = 0.807$
Significance for r[a]		$P = 0.028$

[a]Significance of correlation was determined by the two-tailed *t*-test on Pearson's coefficient (r).

or PMA treatment causes PKC activation and local PIP2 clustering by the PKC substrates, which upholds actin polymerisation, reduction in the G-actin level and elevation in actin expression. In the unloading condition, these processes would be reversed, with down regulation in the PKC signalling pathway and actin expression. An integrative study including mechanotransduction, associated signalling and capping should be approached to comprehend the detailed mechanism of the PKC activation to actin expression connection. In cardiac and smooth cells, mechanical stimulus was reported to induce expression of the skeletal α-actin gene, or actin polymerisation that increased the ratio of fibrous actin:G-actin, possibly via PKC activation [Komuro et al., 1991; Yazaki et al., 1993; Poussard et al., 2001; Cipolla et al., 2002]. We did not study the role of PKCα phosphorylation on myosin protein expression, although this issue also needs clarification. From the literature and other investigations, the phosphorylated form of PKC is considered to be the active form that binds to the cell membranes (see, Gutkind [1998] for review). In our present study, we measured PKC phosphorylation in soleus whole-tissue extract because we were unable to obtain sufficient amounts of sarcolemmal extract from the tissue at these ages of rats. It will be informative to investigate PKCα phosphorylation using subcellular fractionation followed by immunoblotting or immunofluorescence microscopy using a phospho-PKC-specific antibody. Taken together, these results imply that PKCα may play a critical role in linking external loading stress to the regulated expression of α-sarcomeric actin (and thus to muscle tension). To clarify the role of PKCα activation on muscle tension capacity, we will further address the effect of PKC activation on muscle tension using PMA.

It is worth noting a study of Sneddon et al. [2000] that addressed the preventive effect of clenbuterol (a β-adrenergic agonist) on denervation-induced muscle atrophy, a system that represents a good comparison to our current study. These investigators showed that the level of PKCα phosphorylation increases upon denervation of the rat soleus muscle (where the 'passive' stretch is intact), and a further increase in phosphorylation upon clenbuterol treatment significantly attenuates atrophy of the denervated tissue. In our present study, the level of PKCα phosphorylation decreased in the unloaded muscle (where the neural input is intact; Fig. 4A and B). Thus, the physical stretch, rather than motor influence per se, seems important to activate this signalling pathway. The increased PKCα activation in the denervated muscle might indicate that this tissue, in the absence of a feedback control, experienced a greater stretch than did the normal muscle. Since the further increase in PKCα phosphorylation (by clenbuterol treatment) ameliorated muscle atrophy, PKCα activation may be important to maintain myofibrillar constituents or increase the efficiency of mRNA translation [Sneddon et al., 2000].

In addition to PKC activation, MAPK cascades also convert mechanical stimuli into relevant intracellular responses [Long et al., 2004]. We observed differential activation of three kinds of MAPKs, particularly during the reloading period (Fig. 5). From the viewpoint of mechanical stress, reloading and exercise represent comparable loading stimuli because both cases render the tissue 'overloaded' following either unloading or rest. Previous reports show that JNK activity in human or rat skeletal muscle increases 6–15 fold above the basal level after exercise or sciatic-stimulated muscle contraction [Aronson et al., 1997; Boppart et al., 1999, 2000]. These studies also demonstrate that activation of JNK reaches a maximum after 15 min of contraction and remains elevated for about 1 h. This pattern of JNK activation is comparable to that of the soleus muscle during early reloading (Fig. 5A). Thus, activation of JNK signalling is transient for the first several hours of muscle activity, and may reflect a resistance response of the soleus muscle against cellular damage or lesion.

Several studies also show that mechanical stimuli activate the other two MAPKs (ERK and p38) in skeletal muscles. For instance, ERK was activated at a maximum level (15–31 fold over basal level) in 10–30 min during sciatic stimulation or cycling exercise, and remained elevated throughout the 1-h exercise period [Widegren et al., 2001]. Similarly, p38 MAPK activity increased 2.2 fold above the control and remained elevated throughout the 1-h exercise. In addition, Boppart et al. [2000] demonstrated that among p38 isoforms (α, β and γ) in skeletal muscle, p38γ had the highest response (4 fold increase in activity) immediately after exercise but returned to the basal level at 1 day post-

exercise. We also observed relatively moderate activation (2 fold) of p38 for at least 1 day after reloading.

Molecular links between PKC and MAPK pathways in response to unloading have been poorly understood in skeletal muscle, but recent data from various systems are worth noting. In the exercising muscle, a PKC–ERK signalling pathway was found to be involved in the stimulation of hormone-sensitive lipase for triacylglycerol catabolism [Donsmark et al., 2003; Langfort et al., 2003; Long et al., 2004]. Furthermore, accelerated glucose transport upon exercise is likely to be regulated by Ca^{2+}-sensitive cPKC-mediated signalling, in which p38 MAPK may be involved [Widegren et al., 2001]. In differentiating skeletal muscle, down regulation of PKCs (mostly PKCα) increased JNK activation but decreased the activation of the ERK and p38 pathways [Goel and Dey, 2002]. Also, both the PKC–ERK and PKC–p38 MAPK pathways are important in mediating hypertrophy and the migration of smooth muscle cells upon mechanical stress, although their responses depend on the duration and magnitude of the stress [Li and Xu, 2000]. In the case of the cardiac hypertrophic response, elevated contractile output of myocytes increased the activation of the PKC–ERK pathway but not the activation of JNK or p38 [Sugden, 2001]. These results and our findings suggest that the ERK pathway is more likely related to the activation of PKCα for energy mobilisation or cell differentiation, whereas the JNK pathway may be negatively associated with PKCα activation, possibly during the injury-evoking process. The activation pattern of p38 MAPK, and its association with PKCα, seems to be intermediary between JNK and ERK.

In conclusion, our data demonstrate that PKCα may play a principle role in linking external stimuli with the expression of contractile proteins, which then determines the level of twitch exertion. Differential activation of MAPKs may also be important for protecting myofibres against damage during early reloading, mobilising energy sources or regulating the expression of contractile proteins. Because the acute effects of unloading on activation of these molecules cannot be ruled out, this issue needs to be further addressed, particularly with regard to elucidating the potential reversibility of signalling mechanisms during unloading versus reloading. Moreover, as recent studies on exercise have revealed that atypical PKCs mediate MAPK activation [Chen et al., 2002; Rose et al., 2004], future research should address the involvement of diverse PKC isoforms in signal transduction upon unloading. The findings of our study may provide valuable information to aid the search for measures to counter muscle contractile depression in space microgravity or extended periods of bed rest.

ACKNOWLEDGMENTS

We thank Dr. Marni Boppart at University of Illinois—Urbana Champaign and professor Un Jin Zimmerman at University of Pennsylvania for critically reviewing this manuscript, Mr. Suk Kim for processing EM micrographs and Dr. Timothy Taylor for editing the manuscript.

REFERENCES

Adams GR, Caiozzo VJ, Baldwin KM. 2003. Skeletal muscle unweighting: Spaceflight and ground-based models. J Appl Physiol 95:2185–2201.

Aronson D, Dufresne SD, Goodyear LJ. 1997. Contractile activity stimulates the c-Jun NH_2-terminal kinase pathway in rat skeletal muscle. J Biol Chem 272:25636–25640.

Baewer DV, Hoffman M, Romatowski JG, Bain JL, Fitts RH, Riley DA. 2004. Passive stretch inhibits central corelike lesion formation in the soleus muscles of hindlimb-suspended unloaded rats. J Appl Physiol 97:930–934.

Baldwin KM. 1996. Effect of spaceflight on the functional, biochemical, and metabolic properties of skeletal muscle. Med Sci Sports Exerc 28:983–987.

Bittner MA, Holz RW. 2005. Phosphatidylinositol-4,5-bisphosphate: Actin dynamics and the regulation of ATP-dependent and -independent secretion. Mol Pharmacol 67:1089–1098.

Boczan J, Boros S, Mechler F, Kovacs L, Biro T. 2000. Differential expressions of protein kinase C isozymes during proliferation and differentiation of human skeletal muscle cells in vitro. Acta Neuropathol (Berl) 99:96–104.

Boppart MD, Aronson D, Gibson L, Roubenoff R, Abad LW, Bean J, Goodyear LJ, Fielding RA. 1999. Eccentric exercise markedly increases c-Jun NH(2)-terminal kinase activity in human skeletal muscle. J Appl Physiol 87:1668–1673.

Boppart MD, Asp S, Wojtaszewski JF, Fielding RA, Mohr T, Goodyear LJ. 2000. Marathon running transiently increases c-Jun NH_2-terminal kinase and p38 activities in human skeletal muscle. J Physiol 526(Pt 3):663–669.

Cain DF, Infante AA, Davies RE. 1962. Chemistry of muscle contraction: Adenosine triphosphate and phosphoylcreatine as energy suppliers for single contractions of working muscle. Nature 196:214–217.

Caiozzo VJ, Haddad F, Baker MJ, Herrick RE, Prietto N, Baldwin KM. 1996. Microgravity-induced transformations of myosin isoforms and contractile properties of skeletal muscle. J Appl Physiol 81:123–132.

Chen HC, Bandyopadhyay G, Sajan MP, Kanoh Y, Standaert M, Farese RV, Jr., Farese RV. 2002. Activation of the ERK pathway and atypical protein kinase C isoforms in exercise- and aminoimidazole-4-carboxamide-1-beta-D-riboside (AICAR)-stimulated glucose transport. J Biol Chem 277:23554–23562.

Cipolla MJ, Gokina NI, Osol G. 2002. Pressure-induced actin polymerization in vascular smooth muscle as a mechanism underlying myogenic behavior. FASEB J 16:72–76.

Donovan N, Becker EB, Konishi Y, Bonni A. 2002. JNK phosphorylation and activation of BAD couples the stress-activated signaling pathway to the cell death machinery. J Biol Chem 277:40944–40949.

Donsmark M, Langfort J, Holm C, Ploug T, Galbo H. 2003. Contractions activate hormone-sensitive lipase in rat muscle by protein kinase C and mitogen-activated protein kinase. J Physiol 550:845–854.

Fitts RH, Riley DR, Widrick JJ. 2001. Functional and structural adaptations of skeletal muscle to microgravity. J Exp Biol 204:3201–3208.

Goel HL, Dey CS. 2002. PKC-regulated myogenesis is associated with increased tyrosine phosphorylation of FAK, Cas, and paxillin, formation of Cas–CRK complex, and JNK activation. Differentiation 70:257–271.

Gutkind JS. 1998. The pathways connecting G protein-coupled receptors to the nucleus through divergent mitogen-activated protein kinase cascades. J Biol Chem 273: 1839–1842.

Hilgenberg L, Yearwood S, Milstein S, Miles K. 1996. Neural influence on protein kinase C isoform expression in skeletal muscle. J Neurosci 16:4994–5003.

Hornberger TA, Esser KA. 2004. Mechanotransduction and the regulation of protein synthesis in skeletal muscle. Proc Nutr Soc 63:331–335.

Ikebe M, Brozovich FV. 1996. Protein kinase C increases force and slows relaxation in smooth muscle: Evidence for regulation of the myosin light chain phosphatase. Biochem Biophys Res Commun 225:370–376.

Ingber DE. 2003. Mechanobiology and diseases of mechanotransduction. Ann Med 35:564–577.

Isfort RJ, Wang F, Greis KD, Sun Y, Keough TW, Farrar RP, Bodine SC, Anderson NL. 2002. Proteomic analysis of rat soleus muscle undergoing hindlimb suspension-induced atrophy and reweighting hypertrophy. Proteomics 2:543–550.

Komuro I, Katoh Y, Kaida T, Shibazaki Y, Kurabayashi M, Hoh E, Takaku F, Yazaki Y. 1991. Mechanical loading stimulates cell hypertrophy and specific gene expression in cultured rat cardiac myocytes. Possible role of protein kinase C activation. J Biol Chem 266:1265–1268.

Korzick DH, Laughlin MH, Bowles DK. 2004. Alterations in PKC signaling underlie enhanced myogenic tone in exercise-trained porcine coronary resistance arteries. J Appl Physiol 96:1425–1432.

Langfort J, Donsmark M, Ploug T, Holm C, Galbo H. 2003. Hormone-sensitive lipase in skeletal muscle: Regulatory mechanisms. Acta Physiol Scand 178:397–403.

Laux T, Fukami K, Thelen M, Golub T, Frey D, Caroni P. 2000. GAP43, MARCKS, and CAP23 modulate PI(4,5)P(2) at plasmalemmal rafts, and regulate cell cortex actin dynamics through a common mechanism. J Cell Biol 149:1455–1472.

Lee M, Choi I, Park K. 2002. Activation of stress signaling molecules in bat brain during arousal from hibernation. J Neurochem 82:867–873.

Lee K, Lee YS, Lee M, Yamashita M, Choi I. 2004. Mechanics and fatigability of the rat soleus muscle during early reloading. Yonsei Med J 45:690–702.

Li C, Xu Q. 2000. Mechanical stress-initiated signal transductions in vascular smooth muscle cells. Cell Signal 12:435–445.

Liu JP. 1996. Protein kinase C and its substrates. Mol Cell Endocrinol 116:1–29.

Long YC, Widegren U, Zierath JR. 2004. Exercise-induced mitogen-activated protein kinase signalling in skeletal muscle. Proc Nutr Soc 63:227–232.

Lyubimova A, Bershadsky AD, Ben-Ze'ev A. 1997. Autoregulation of actin synthesis responds to monomeric actin levels. J Cell Biochem 65:469–478.

Nyhan D, Kim S, Dunbar S, Li D, Shoukas A, Berkowitz DE. 2002. Impaired pulmonary artery contractile responses in a rat model of microgravity: Role of nitric oxide. J Appl Physiol 92:33–40.

Poussard S, Dulong S, Aragon B, Jacques Brustis J, Veschambre P, Ducastaing A, Cottin P. 2001. Evidence for a MARCKS–PKCalpha complex in skeletal muscle. Int J Biochem Cell Biol 33:711–721.

Riley DA, Bain JL, Thompson JL, Fitts RH, Widrick JJ, Trappe SW, Trappe TA, Costill DL. 2000. Decreased thin filament density and length in human atrophic soleus muscle fibers after spaceflight. J Appl Physiol 88:567–572.

Rose AJ, Michell BJ, Kemp BE, Hargreaves M. 2004. Effect of exercise on protein kinase C activity and localization in human skeletal muscle. J Physiol 561: 861–870.

Sneddon AA, Delday MI, Maltin CA. 2000. Amelioration of denervation-induced atrophy by clenbuterol is associated with increased PKC-alpha activity. Am J Physiol Endocrinol Metab 279:E188–E195.

Sugden PH. 2001. Signalling pathways in cardiac myocyte hypertrophy. Ann Med 33:611–622.

Tanaka S, Kanaya N, Homma Y, Damron DS, Murray PA. 2002. Propofol increases pulmonary artery smooth muscle myofilament calcium sensitivity: Role of protein kinase C. Anesthesiology 97:1557–1566.

Vandenburgh H, Chromiak J, Shansky J, Del Tatto M, Lemaire J. 1999. Space travel directly induces skeletal muscle atrophy. FASEB J 13:1031–1038.

Widegren U, Ryder JW, Zierath JR. 2001. Mitogen-activated protein kinase signal transduction in skeletal muscle: Effects of exercise and muscle contraction. Acta Physiol Scand 172:227–238.

Yazaki Y, Komuro I, Yamazaki T, Tobe K, Maemura K, Kadowaki T, Nagai R. 1993. Role of protein kinase system in the signal transduction of stretch-mediated protooncogene expression and hypertrophy of cardiac myocytes. Mol Cell Biochem 119:11–16.